

Nanocomposite polymer carbon-black coating for triggering pyro-electrohydrodynamic inkjet printing

S. Coppola,¹ L. Mecozzi,^{1,2,a)} V. Vespini,¹ L. Battista,¹ S. Grilli,¹ G. Nenna,³ F. Loffredo,³ F. Villani,³ C. Minarini,³ and P. Ferraro¹

¹CNR-Institute of Applied Sciences & Intelligent Systems “E. Caianiello,” via Campi Flegrei 34, 80078 Pozzuoli (NA), Italy

²Università degli Studi di Napoli “Federico II,” Facoltà di Ingegneria P.le Tecchio 80, 80125 Napoli, Italy

³ENEA-Portici Research Center, Piazzale Enrico Fermi, 1, 80055 Portici (NA), Italy

(Received 30 April 2015; accepted 23 June 2015; published online 30 June 2015)

The pyro-electrohydrodynamic (EHD) manipulation of liquids has been discovered and demonstrated recently as a high resolution printing technique avoiding the use of nozzles and external electrodes. The activation of the pyro-electric effect is usually achieved on ferroelectric crystals by an external heating source or by an infrared laser. Here, we show an original modality for triggering the pyro-EHD process through a light-absorbing polymer nanocomposite thin layer deposited on the ferroelectric substrate, thus overcoming some limitations of the previous configuration. Significant simplification and compactness of the set-up is achieved thanks to the nanocomposite coating, since a commercial low-cost white-light halogen lamp can be adopted to trigger the pyro-jetting process from a liquid reservoir. Remarkably, high resolution is achieved in dispensing very high viscous liquids. Practical demonstrations in polymer optical microlenses direct printing using polydimethylsiloxane and poly(methyl methacrylate) are finally reported to validate the approach in handling high-viscous polymers for practical applications. © 2015 AIP Publishing LLC.

[<http://dx.doi.org/10.1063/1.4923469>]

Actually, the manipulation of liquids and nano-objects is very attractive with important applications in biotechnology, photonics, and micro-opto-electro-mechanical systems.^{1–4} Even today, in micro and nanoscience, one of the most common difficulties consists in handling little droplets and controlling their movement for high resolution patterning and on demand printing.^{5,6} Different nanofluidic capabilities have been promoted for manipulating and dispensing polymers droplets, but all of them are based on the use of multiple components, such as channels, syringes, or nozzles, where the liquid of interest is transported and then released.^{7,8} More recently, electrohydrodynamic (EHD) jetting⁹ has been used for drawing thin jets of liquids from fine apertures.¹⁰ A number of techniques have been proposed for the actuation of microfluidic droplets based on thermocapillary effects,¹¹ electrochemical gradients,¹² photochemical effects,¹³ or optoelectronic-induced electrokinetics.¹⁴ In comparison with the conventional ones, actually, the EHD ink-jet printing technique could guarantee high-resolution and on-demand patterning of functional materials in liquid form.⁵ Regarding polymers handling, e.g., for the fabrication of optical components, EHD provides advantages in capabilities over conventional ink-jet approaches, but at the same time complex set-up including high-voltage generators, external electrodes, and additional micro components are needed.^{15–18} Recently, an alternative technology, named pyro-EHD printing,^{18–22} has been discovered. The pyro-EHD allows to manipulate liquids in a no-contact mode and avoids the use of nozzles and external electrodes, thus

overcoming some severe limitations of ink-jet printing, like, for example, nozzle-clogging.²³ Even if the pyro-EHD approach adds important advantages in processing functional materials by simply applying a temperature gradient onto a pyro-electric crystal, some limitations are still encountered in printing small volumes of polymers at high resolution.²² In fact, some polymers like polydimethylsiloxane (PDMS) and poly(methyl methacrylate) (PMMA), which are commonly employed in different fields of technology from electronic to biomicrofluidics, are very difficult to dispense even by pyro-EHD. Here, we propose an innovative method for the activation of the pyro-EHD inkjet system that allows the handling of very high viscous polymers and their direct printing. In the proposed configuration, the pyro-electric effect is enhanced using a carbon black-based nanocomposite coating directly applied on the substrate (Lithium Niobate, LN). The pyro-EHD process is triggered efficiently by a halogen lamp, allowing high extraction force for PDMS and PMMA microlenses direct printing. The proposed apparatus introduces a further significant simplification when compared to the standard configuration of the “pyro-EHD dispenser”¹⁸ or the pyro-Thetered-Electrospinning^{24,25} thus making the system versatile, more compact, and low cost in order to produce integrated systems.

The pyro-jetting effect is simply activated by a temperature gradient directly applied onto ferroelectric crystals.¹⁸ The introduction of a coating based on carbon structures (carbon black—CB, multiwall carbon nanotubes—MWCNTs, and graphene nanoparticles) on the top of LN or LT crystals can improve their radiation absorption^{26–28} maximizing the resulting rise in temperature per unit of incident radiant power. In particular, the use of radiation absorbing coatings

^{a)}Author to whom correspondence should be addressed. Electronic mail: l.mecozzi@cib.na.cnr.it

is determinant in the visible range (crystal are transparent from 320 to 5000 nm, Refs. 29 and 30), improving the efficiency and involving the whole visible and IR wavelengths, as demonstrated for energy harvesting.³¹

The fabrication process used to produce a nanocomposite coating to be applied on the z-face of LN crystals is diagrammed in Figures 1(a)–1(d). The method consists in the preparation of a PDMS/CB film on Polyvinyl Alcohol (PVA)-coated glass substrate followed by its peeling from the substrate and by the subsequent application of the resulting PDMS/CB membrane directly at a later stage to the crystal. In detail, the glass substrate, a microscope coverslip, was functionalized by spin-coating a PVA solution (2.8% in water) at 2000 rpm for 2 min. This step was repeated four times to produce a film thick enough to allow the easy peeling of the membrane (Figure 1(a)). Then, a CB suspension was prepared in PDMS (Figure 1(b)) by adding 0.02 g of CB (graphitized CB-carbon nanopowder, size <200 nm, >99.95%) in 0.5 g of PDMS curing agent (Dow Corning Sylgard 184; 10:1 prepolymer to curing agent) and sonicating it for 2 h. A drop of the suspension obtained after adding the elastomeric base to the solution was finally deposited on the top of the PVA-coated coverslip and cured at room temperature for 12 h. Once the CB membrane was peeled-off from the coverslip (Figure 1(c)), it was set down on the crystal (Figure 1(d)).

Despite of the various methods presented in literature,^{32–34} we focused on a pyro-EHD dispensing method¹⁸ particularly attractive for the direct writing of materials from liquid drop. The system is simplified with respect to the conventional ink-jet apparatus and consists of just two plates and a halogen Osram lamp used as heating source (focal length 32.0 mm, 12 V, and 75 W) and operating on the CB coated crystals (Figure 1(e)). The set-up could be mounted in a static or dynamic configuration. In both cases, the upper plate is constituted of a microscope coverslip, used as receiving substrate, placed on a three-axes translation stage, while the CB coated LN crystal drives the process. In the static configuration, the collector is fixed in space, so that the reservoir drop can dispense multiple jetting in the same position increasing the dimension, in terms of volume and geometric characteristics, of the deposited droplet. On the other hand, one more interesting configuration is related to the continuous printing of separate droplets and this is possible just controlling the movement of the target substrate with high precision motorized positioners. The distance between the

two plates was set on the scale of the hundreds of microns depending on the investigated base drop. The experienced thermal gradient using the configuration including a uniform CB membrane ($2 \times 2 \text{ cm}^2$) was enhanced with respect to previous works.³¹ Indeed, it can be possible to realize patterned coating membrane so allowing the selective activation of the pyro-electric field. This configuration could increase the possibility of using the presented nozzle-less approach, especially in case of multiple starting drop, for the direct writing of arrays or matrices. We start focusing on the activation of a single drop as depicted in Figure 1(d). A video camera was used to monitor the printing process; the light coming from a collimated LED light source (Thorlabs M470L2) illuminates the cross section of the dispensing system, then it is collected by a $10\times$ microscope objective and finally projected onto a CMOS camera (Motion Pro Y3-S1). Depending on the material of the reservoir drop, the dynamic and the jetting evolution could be different. In order to prove the use of the pyro-jetting method for direct printing polymer materials and overcoming the viscosity limit of conventional ink-jet apparatus;²³ in our experiments, we used as base drops, PMMA and PDMS with different viscosities (PDMS: 3500 cps and PMMA: 560 cps). The manipulation of PDMS with the “pyro-dispenser”¹⁸ still suffer of some limitations. As shown in Figure 2(a), the starting polymer drop assumes the shape of a liquid bridge that comes in contact with the target substrate and in this condition the dispensing of polymer drops is impracticable. On contrary, by introducing a CB coating, the pyro-effect is enhanced so that the polymer drop deforms into a sharp and elongated Taylor cone from which tiny amount of polymer could be dispensed. In fact, the use of a CB-layer reduces the recombination of the temporary surface charges and decreases the heat transfer from the crystal to the air, thus increasing the temperature gradient and improving the pyro-electric efficiency.^{18,24} Furthermore, also the geometry of electric field lines plays a role in the process: they appear different in case of a confined heating area with respect to an extended one. The plots of electric field lines for localized heating and for uniform heating with a CB-layer are shown in Figures 2(a) and 2(b), respectively. It can be noted that when a CB-layer is used, the electric field is very uniform over a large area, thus affecting the geometry of the dispensing process. The thickness of the CB-layer is about $200 \mu\text{m}$; this value is the result of an easy method of preparation and peeling for a uniform CB membrane,

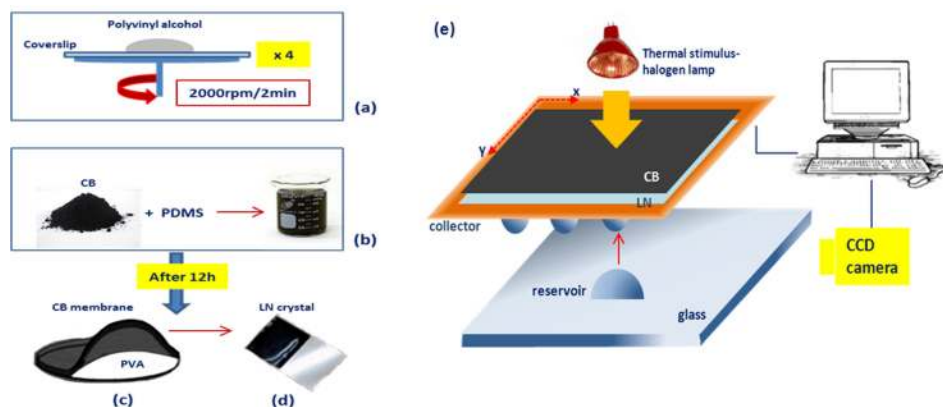


FIG. 1. (a)–(d) Schematic diagram of the CB deposition process and (e) pyro-EHD set-up using the halogen lamp as the heating source.

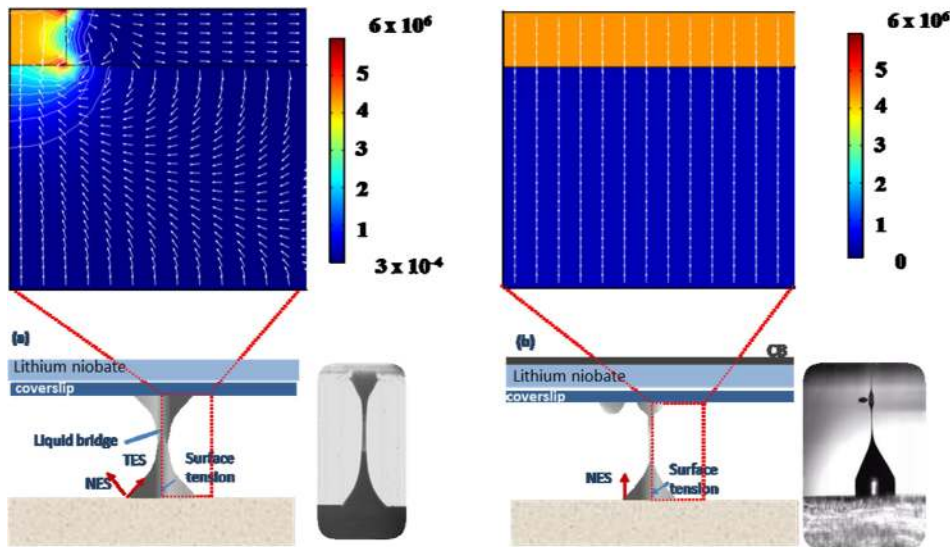


FIG. 2. Images of the PDMS-based reservoir drop deformation obtained by standard pyro-effect configuration (a) and innovative pyro-effect configuration employing a CB coating. In the case (a) the starting polymer drop assumes the shape of liquid bridge and experiences both normal and tangential components of the stress tensor while by introducing a CB coating (b) the pyro-effect is enhanced so that the polymer drop deforms into a sharp and elongated printing cone under the action of the tangential components.

balanced with the radiation absorption valuable for the activation of the pyro-electric effect. The EHD force generated at the interface air-polymer can be represented by a stress tensor, with normal and tangential components. In Figure 2(a), under the influence of the pyro-electric field, the air-polymer interface moves dynamically while in case of Figure 2(b) it appears uniform and experiences a stress tensor with a single component. In this case, once the pyro-electric field is applied, the top polymer surface moves progressively upward with a spatially non uniform geometry; the elongated cone experiences a greater EHD force under a small distance, thus leading to the activation of the upper surface and to the formation of a thin polymer tip.⁷

The pyro-electric effect was exploited through the CB-coated system for the fabrication on demand of single droplets characterized as lenses and microlenses arrays. PDMS and PMMA were chosen because of their good optical and mechanical properties. PDMS was used without any dilution,

while the PMMA ink was prepared by dissolving 200 mg/ml of PMMA ($M_w = 120\,000$ a.m.u) in pure N-Methyl-2-pyrrolidone (NMP). We prepared the PDMS and PMMA inks in the same conditions tested for the pyro-EHD printing systems in order to better compare the results obtained.^{19,20} In particular, referring to the PMMA ink, we chose the better condition of use found in our previous work²² where various solutions at different mixing ratio of polymer and solvent have been tested. The receiving substrate was previously functionalized by means of a hydrophobic tetra-ethylorthosilicate/1H,1H,2H,2H-perfluorodecyl-triethoxysilane (TEOS/PFTEOS) film, spin-coated from a sol-gel solution in order to minimize the spreading of the dispensed droplets. In Figure 3(a), we report the microscope image and the corresponding two dimensional profile (analyzed by DektakXT–Bruker system) of a single PMMA microlens obtained in static configuration. In Figure 3(b), we show examples of PDMS microstructures, specifically a single lens obtained in static configuration and

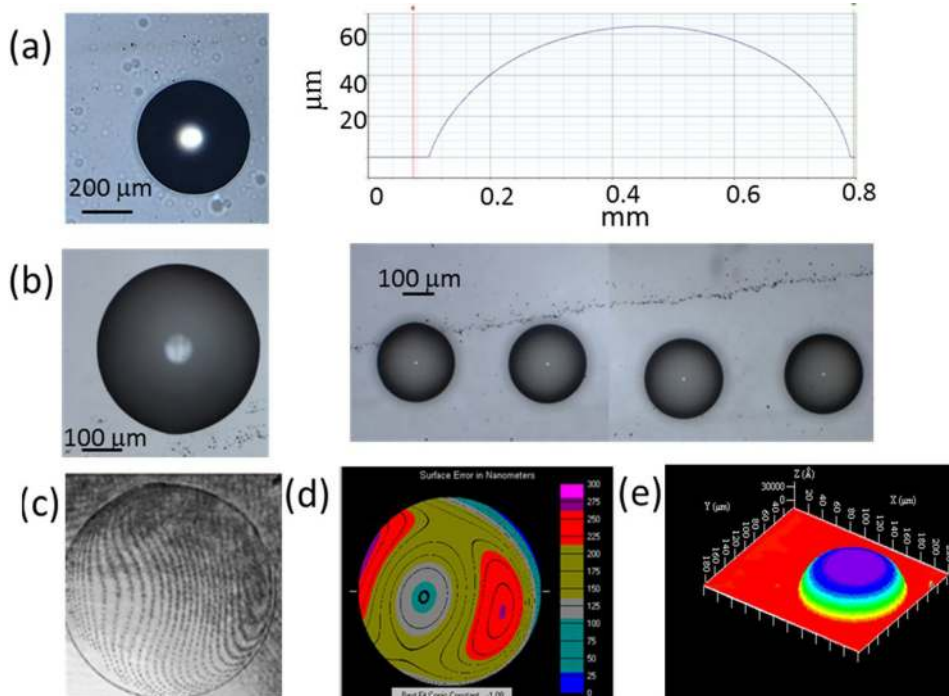


FIG. 3. (a) Single PMMA microlens and corresponding profile, (b) PDMS microlens (left) and linear array of multiple lenses (right). Tilted interferometric fringe image (c), wavefront error (d), and 3D image of the PMMA microlenses (e).

an array of multiple lenses produced in dynamic mode. Controlling the experimental conditions and the starting droplet, we were able to produce PDMS lenses with different diameters ranging from 50 to 700 μm .

The optical and geometrical characterizations were carried out through the interferometric technique. The resulting interference pattern contains quantitative information derived from the shape of the fringes and the space between the fringes themselves. In case of the PMMA microlenses, the complete optical and geometrical characterization was performed by means of a Mach-Zehnder system in confocal configuration. The single-path interferometer was preferred to the double-path one (e.g., Michelson and Twyman–Green interferometers) in order to minimize the measurement errors due to the used optical components.³⁵ A fringe analysis software was used to analyze the detected interference pattern (Figure 3(c)). The first step in the analysis was to plot data points along the fringes. The relative positions of each point provide the information about the microlens shape and the relative optical quality. The modelling process by means of the fringe analysis software uses Zernike polynomials to describe aberrations of lenses from an ideal spherical shape, which results in refraction errors.^{36,37} The results obtained show that all the realized microlenses are aspheric and, in particular, they have a parabolic morphology. These geometrical features were confirmed by profilometric 3D analysis, as visible in Fig. 3(e), where the geometrical properties of the lens are 128 μm diameter and 12 μm height, respectively. Due to the final aspheric shape of the lens, which consists in an ellipsoidal base (along xy-plane) and parabolic shape in the other direction (along z-axis), the evaluation of the focal length was very complex and it was possible to evaluate it in the range of 1.2 and 1.4 mm. In particular, according to the formula $Z^2 - 2RX + (K + 1)X^2 = 0$, $K \sim -1$, where K is the conic constant in accordance with the parabolic shape and R is the radius of curvature. In particular, in order to better evaluate the focal length for the PDMS lenses, the analysis was performed using the Axio Imager-M1 Zeiss microscope as described in the supplementary material.³⁸ In this case, the focal length increases for larger lens diameters achieving the value of about 1200 μm for a diameter of 600 μm . In order to reduce the geometrical characteristics of the lenses (diameter of tens of microns), we studied an alternative controllable self-assembly approach onto a hydrophobic substrate for a large-scale production of microlenses arrays. The material used in the experiment, described in the supplementary material,³⁸ is a high viscous biopolymer, poly (lactico-glycolic acid, 3200 cps) PLGA and the self-assembled dot arrays produced could be employed in bio-inspired applications.

In summary, the dispensing of separate polymer drops is achieved through a smart simplification of the nozzle-less pyro-EHD dispenser set-up, where a commercial halogen lamp illuminates the nanocomposite polymer CB layer onto the LN crystals surface in order to induce the pyro-electric effect. The improvement of properties and functionalities of the EHD printing process has been reported. Different experiments were conducted to prove the use of high viscous polymers (PDMS, PMMA, and PLGA). It is shown that dispensed polymer drops can be adopted as microlenses. In fact, the presented results, supported by profilometric and

interferometric analyses, demonstrate the feasibility to obtain optical microlenses through this innovative nozzle-free technique in the focal range of 1.2 and 1.4 mm and diameter from 70 to 700 μm while the production of micro-array in PLGA for microchemical reaction, DNA detection, and biosensing could be foreseen.

This work was supported by RELIGHT (research for light PON02_00556_3306937), the EFOR-CABIR CNR, and by the MAAT project. The authors also acknowledge the Italian Ministry of Research for financial support, under the “Progetto Operativo Nazionale” Pandion (PON01_00375).

- ¹V. Taly, B. T. Kelly, and A. D. Griffiths, *ChemBioChem* **8**, 263 (2007).
- ²T. M. Squires and S. R. Quake, *Rev. Mod. Phys.* **77**, 977 (2005).
- ³B. Y. Ahn, E. B. Duoss, M. J. Motala, X. Y. Guo, S. I. Park, Y. J. Xiong, J. Yoon, R. G. Nuzzo, J. A. Rogers, and J. A. Lewis, *Science* **323**, 1590 (2009).
- ⁴J.-U. Park, M. Hardy, S. J. Kang, K. Barton, K. Adair, D. K. Mukhopadhyay, C. Y. Lee, M. S. Strano, A. G. Alleyne, J. G. Georgiadis, P. M. Ferreira, and J. A. Rogers, *Nat. Mater.* **6**, 782 (2007).
- ⁵J.-U. Park, S. Lee, S. Unarunotai, Y. Sun, S. Dunham, T. Song, P. M. Ferreira, A. G. Alleyne, U. Paik, and J. A. Rogers, *Nano Lett.* **10**, 584 (2010).
- ⁶F. D. Prasetyo, H. T. Yudistira, V. DatNguyen, and D. Byun, *J. Micromech. Microeng.* **23**, 095028 (2013).
- ⁷B. de Heij, M. Daub, O. Gutmann, R. Niekravietz, H. Sandmaier, and R. Zengerle, *Anal. Bioanal. Chem.* **378**, 119 (2004).
- ⁸T. Ondarçuhu, J. Arcamone, A. Fang, H. Durou, E. Dujardin, G. Rius, and F. Pérez-Murano, *Eur. Phys. J. Spec. Top.* **166**, 15 (2009).
- ⁹L. T. Cherney, “Structure of Taylor cone-jets: Limit of low flow rates,” *J. Fluid Mech.* **378**, 167 (1999).
- ¹⁰R. T. Collins, J. J. Jones, M. T. Harris, and O. A. Basaran, *Nat. Phys.* **4**, 149 (2008).
- ¹¹M. A. Burns, C. H. Mastrangelo, T. S. Sammarco, F. P. Man, J. R. Webster, B. N. Johnsons, B. Foerster, D. Jones, Y. Fields, A. R. Kaiser, and D. T. Burke, *Proc. Natl. Acad. Sci. U.S.A.* **93**, 5556 (1996).
- ¹²B. S. Gallardo, V. K. Gupta, F. D. Egerton, L. I. Jong, V. S. Craig, R. R. Shah, and N. L. Abbott, *Science* **283**, 57 (1999).
- ¹³K. Ichimura, S.-K. Oh, and M. Nakagawa, *Science* **288**, 1624 (2000).
- ¹⁴P. Y. Chiou, A. T. Ohta, and M. C. Wu, *Nature* **436**, 370 (2005).
- ¹⁵F. F. Wang, F. Fei, L. Q. Liu, H. B. Yu, P. Yu, Y. C. Wang, G. B. Lee, and W. Jung, *Appl. Phys. Lett.* **104**, 264103 (2014).
- ¹⁶C. H. Ru, J. Luo, S. R. Xie, and Y. Sun, *J. Micromech. Microeng.* **24**, 053001 (2014).
- ¹⁷Y. Kim, S. Jang, and J. H. Oh, *Appl. Phys. Lett.* **106**, 014103 (2015).
- ¹⁸P. Ferraro, S. Coppola, S. Grilli, M. Paturzo, and V. Vespini, *Nat. Nanotechnol.* **5**, 429 (2010).
- ¹⁹V. Vespini, S. Coppola, S. Grilli, M. Paturzo, and P. Ferraro, *Lab Chip* **11**, 3148 (2011).
- ²⁰S. Coppola, V. Vespini, S. Grilli, and P. Ferraro, *Lab Chip* **11**, 3294 (2011).
- ²¹I. A. Grimaldi, S. Coppola, F. Loffredo, F. Villani, C. Minarini, V. Vespini, L. Miccio, S. Grilli, and P. Ferraro, *Opt. Lett.* **37**, 2460 (2012).
- ²²I. A. Grimaldi, S. Coppola, F. Loffredo, F. Villani, G. Nenna, C. Minarini, V. Vespini, L. Miccio, S. Grilli, and P. Ferraro, *Appl. Opt.* **52**, 7699 (2013).
- ²³D. G. Yu, C. Branford-White, K. White, N. P. Chatterton, L. M. Zhu, L. Y. Huang, and B. Wang, *eXPRESS Polym. Lett.* **5**, 732 (2011).
- ²⁴S. Coppola, V. Vespini, G. Nasti, O. Gennari, S. Grilli, M. Ventre, M. Iannone, P. A. Netti, and P. Ferraro, *Chem. Mater.* **26**, 3357 (2014).
- ²⁵R. Vecchione, S. Coppola, E. Esposito, C. Casale, V. Vespini, S. Grilli, P. Ferraro, and P. A. Netti, *Adv. Funct. Mater.* **24**, 3515 (2014).
- ²⁶E. Theocharous, R. Deshpande, A. C. Dillon, and J. Lehman, *Appl. Opt.* **45**, 1093 (2006).
- ²⁷J. H. Lehman, C. Engtrakul, T. Gennett, and A. C. Dillon, *Appl. Opt.* **44**, 483 (2005).
- ²⁸E. Theocharous, C. Engtrakul, A. C. Dillon, and J. Lehman, *Appl. Opt.* **47**, 3999 (2008).
- ²⁹Z. Lu, K. Zhao, and X. Li, *Ferroelectrics—Physical Effects*, edited by M. Lallart (InTech, Rijeka, Croatia, 2011), Chap. 28.
- ³⁰H. Xia, X. Zeng, J. Wang, J. Zhang, J. Xu, Y. Zhang, and Q. Nie, *Crystr. Res. Technol.* **39**, 337 (2004).

- ³¹L. Battista, L. Mecozzi, S. Coppola, V. Vespini, S. Grilli, and P. Ferraro, *Appl. Energy* **136**, 357 (2014).
- ³²R. Ahmed and T. B. Jones, "Optimized liquid DEP droplet dispensing," *J. Micromech. Microeng.* **17**, 1052 (2007).
- ³³A. Casner and J.-P. Delville, "Laser-induced hydrodynamic instability of fluid interfaces," *Phys. Rev. Lett.* **90**, 144503 (2003).
- ³⁴Y. A. Huang, N. B. Bu, Y. Q. Duan, Y. Q. Pan, H. M. Liu, Z. P. Yin, and Y. L. Xiong, *Nanoscale* **5**(24), 12007 (2013).
- ³⁵H. M. Tian, J. Y. Shao, Y. C. Ding, X. M. Li, and H. Z. Liu, *Langmuir* **29**, 4703 (2013).
- ³⁶I. A. Grimaldi, A. De Girolamo Del Mauro, F. Loffredo, G. Nenna, F. Villani, and C. Minarini, *Proc. SPIE* **8082**, 808244 (2011).
- ³⁷M. S. Kim, T. Scharf, and H. P. Herzig, *Opt. Express* **18**, 14319 (2010).
- ³⁸See supplementary material at <http://dx.doi.org/10.1063/1.4923469> for characterization of "Focal lengths of PDMS microlenses" and "Patterning of PLGA microstructures."